Computers and Concrete, Vol. 11, No. 1 (2013) 21-37
DOI: http://dx.doi.org/10.12989/cac.2013.11.1.021

Shear behavior of reinforced HPC beams made of a low cement content without shear reinforcements

Chao-Wei Tang[*1], Yu-Ping Chen[2], How-Ji Chen[3], Chung-Ho Huang[4] and Tsang-Hao Liu[5]

[1]*Department of Civil Engineering & Engineering Informatics, Cheng Shiu University, No. 840, Chengcing Rd., Niaosong District, Kaohsiung Cinty, Taiwan R.O.C.*
[2]*Graduate Institute of Construction Engineering, Cheng Shiu University, No. 840, Chengcing Rd., Niaosong District, Kaohsiung City, Taiwan R.O.C.*
[3]*Department of Civil Engineering, National Chung-Hsing University, No. 250, Kuo Kuang Road, Taichung, Taiwan*
[4]*Department of Civil Engineering, Dahan Institute of Technology*
[5]*AU Optronics Corporation*

(Received March 23, 2011, Revised February 21, 2012, Accepted February 28, 2012)

Abstract. High-performance concrete (HPC) usually has higher paste and lower coarse aggregate volumes than normal concrete. The lower aggregate content of HPC can affect the shear capacity of concrete members due to the formation of smooth fractured surfaces and the subsequent development of weak interface shear transfer. Therefore, an experimental investigation was conducted to study the shear strength and cracking behavior of full-scale reinforced beams made with low-cement-content high-performance concrete (LcHPC) as well as conventional HPC. A total of fourteen flexural reinforced concrete (RC) beams without shear reinforcements were tested under a two-point load until shear failure occurred. The primary design variables included the cement content, the shear span to effective depth ratio (*a/d*), and the tensile steel ratio (ρ_w). The results indicate that LcHPC beams show comparable behaviors in crack and ultimate shear strength as compared with conventional HPC beams. Overall, the shear strength of LcHPC beams was found to be larger than that of corresponding HPC beams, particularly for an *a/d* value of 1.5. In addition, the crack and ultimate shear strength increased as *a/d* decreased or ρ_w increased for both LcHPC beams and HPC beams. This investigation established that LcHPC is recommendable for structural concrete applications.

Keywords: low cement content; high-performance concrete; shear strength; beam.

1. Introduction

High-performance concrete (HPC) is an important innovation in concrete technology. It is not just a high-strength concrete (HSC), and in fact, it has replaced the HSC developed in the early 1980s. HPC is defined as concrete that is made of appropriate materials, such as chemical admixtures and mineral admixtures, which are combined according to a selected mix design, and

[*]Corresponding author, Professor, E-mail: tangcw@csu.edu.tw

that is properly mixed, transported, placed, consolidated and cured to give excellent performance in certain properties of the concrete (Russell 1999). A HPC using cement alone as a binder requires a high paste volume, which often leads to excessive shrinkage and a large evolution of heat during hydration, in addition to an increased cost. A partial replacement of cement by mineral admixtures, such as fly ash or ground granulated blast-furnace slag in concrete mixes, helps to overcome these problems and leads to improvement in the durability of the concrete (Somayaji 2001, Mehta and Monteiro 2006). This replacement also leads to additional benefits in terms of a reduction in cost, energy savings, the promotion of ecological balance and the conservation of natural resources, among others.

In the last few decades, industrial by-products such as fly ash, blast-furnace slag and silica fume have been increasingly used in concrete to replace part of the cement. Moreover, the increased use of mineral admixtures has led to an equivalent reduction of greenhouse gas emissions and represents one of the best technically proven approaches for reducing the cement industry's emissions. Still, it is well recognized that the maximum cement content for ordinary HPC is exceeded by either the cement content needed for concrete strength or the minimum cement content required for durability (Cheng *et al.* 2009, Tang 2010). In other words, there is still ample room for reducing the cement content in concrete to limit the heat of hydration and/or shrinkage.

The shear behavior of reinforced concrete members is generally more complicated than the flexural behavior. The shear characteristics of reinforced concrete members without shear reinforcements have been an especially important part of the information influencing the design process of concrete beams and frames. Therefore, numerous theoretical and experimental studies have concentrated on beams without stirrups (Zsutty 1971, Taylor 1972, Park and Paulay 1975, ENV 1992-1-1: Eurocode No. 2 1991, Rebeiz 1999, Zarais and Papadakis 2001, Cho 2003, Zararis 2003, Russo *et al.* 2005, Bentz 2005, ACI Committee 318 2005, Choi *et al.* 2007, Hassan *et al.* 2008, Tang *et al.* 2009).

Although HPC has been increasingly used in the construction industry during the last decade, most current design codes only cover concrete with strengths up to 50 MPa. An increase in the strength of concrete is directly associated with an improvement in most of its properties, especially the durability, but this also produces an increase in the brittleness and smoother crack surfaces, which significantly affect the shear strength. The impact of the HPC mix proportions on the shear capacity is not yet fully understood for structural applications. Hence, there is a great need to check the practical applications of current regulations.

In view of the above statements, this study tested the shear behavior of longitudinally reinforced LcHPC beams without shear reinforcements with the goal of enhancing the understanding of the behavior of high-strength concrete beams without shear reinforcements those are failing in shear and comparing this with companion HPC beams. A total of fourteen simply supported RC beams were designed for shear failure with a two-point bending system. The concrete compressive strength of the beams at the age of the tests was approximately 69 MPa. The primary design variables included the cement content, the shear span to effective depth ratio (a/d), and the tensile steel ratio (ρ_w). In addition, the test results were also compared with those obtained using empirical shear strength equations available in the literature.

2. Empirical formulae for shear strength

Several design codes and empirical equations in the literature are available for predicting the shear strength of RC beams without shear reinforcements. Some prominent methods are outlined in the following.

The ACI 318-08 code presents two different procedures for calculating the diagonal crack shear strength, V_{cr}, of RC beams without stirrups subjected to shear and flexure loadings. The simplified empirical formula is as follows (ACI Committee 318 2008)

$$V_{cr} = \left(\frac{\sqrt{f_c'}}{6} \right) b_w d \qquad \text{(SI units)}, \tag{1}$$

where b_w = the breadth of the beam, d = the effective depth of the beam, and f_c' = compressive strength of concrete measured on cylinder. The simplified ACI equation is a lower bound for slender beams that are not subjected to axial loading and have at least 1% longitudinal reinforcement. The detailed empirical formula is as follows

$$V_{cr} = \left(0.16\sqrt{f_c'} + 17\rho_w \frac{V_u d}{M_u} \right) b_w d \le 0.3\sqrt{f_c'} b_w d \qquad \text{(SI units)}, \tag{2}$$

where f_c' < 70 MPa, ρ_w = the longitudinal tensile steel ratio, V_u = the factored shear force at the considered section, M_u = the factored moment occurring simultaneously with V_u at the section under evaluation. When computing Eq. (2), V_u/M_u should not be greater than one.

In contrast, deep beams with a length of clear span not exceeding four times the overall member depth can be designed using strut-and-tie methods (STM), as described in Appendix A of the ACI 318-08 Building Code. The components of a typical STM model of a single-span deep beam loaded with a concentrated load, composed of struts and ties connected at nodes, is capable of transferring the factored loads to the supports. The nominal shear strength of a strut without longitudinal reinforcement, V_{ns}, is

$$V_{ns} = f_{ce} A_{cs} \times \sin\theta , \tag{3}$$

where f_{ce} = the effective compressive strength of the concrete in the strut or in the nodal zone, A_{cs} = the cross-sectional area at one end of the strut and θ = the angle between axis of strut and the tension cord of the member. The nominal shear strength of a tie, V_{nt}, is

$$V_{nt} = A_{ts} f_y \times \tan\theta , \tag{4}$$

where A_{ts} = the area of reinforcement in the tie, and f_y = the specified yield strength of the reinforcement. The nominal shear strength of a nodal zone, V_{nn}, is

$$V_{nn} = f_{ce} A_{nz} \times \sin\theta , \tag{5}$$

where f_{ce} = the effective compressive strength of the concrete in the nodal zone, and A_{nz} = the smaller of the areas of the face of the nodal zone and a section through the nodal zone. For deep beams subject to only shear and flexure, therefore, the nominal shear strength V_n may be taken as

$$V_n = Min(V_{ns}, V_{nt}, V_{nn}) . \quad (6)$$

As for the first version of Eurocode EC2 Part 1 (1991), the empirical formula for the shear resistance in non-prestressed members not requiring design stirrups is given by

$$V_{cr} = \tau_{Rd} k_1 \beta (1.2 + 40\rho_w) b_w d \quad \text{(SI units)}, \quad (7)$$

where k_1 = (1.6-d/1000) should not be less than 1.0, β = 1 for $a/d \geq 2.5$ or $\beta = 2.5d/a$ should not be greater than 5 for $a/d < 2.5$, $\rho = A_{sl}/b_w d$ should not be greater than 0.02 (where A_{sl} is the area of the anchored tensile reinforcement), and $\tau_{Rd} = 0.25 f_{ctk0.05}/\gamma_c$ with γ_c =1.5, $f_{ctk0.05} = 0.7 f_{ctm}$, and f_{ctm} =0.3 $f_c^{'2/3}$. Eq. (7) was revised in April 2003. Therefore, the revised empirical formula for the shear resistance is given by (ENV 1992-1-1: Eurocode No. 2 2003)

$$V_{cr} = \left[\frac{0.18}{\gamma_c} k (100 \rho_w f_c^{'})^{1/3} \right] b_w d \geq 0.035 k^{3/2} \sqrt{f_c^{'}} b_w d \quad \text{(SI units)}, \quad (8)$$

where $k = 1+(200/d)^{1/2}$ should not be greater than 2.0.

Rebeiz (1999) presented alternative shear strength prediction equations for steel-reinforced concrete members without shear reinforcements. He used the techniques of dimensional analysis, interpolation function, and multiple regression analysis. The proposed crack and ultimate shear strength prediction equations are given separately as follows

$$V_{cr} = 0.4 b_w d + \sqrt{f_c^{'} \rho_w (d/a)} (2.7 - 0.4 A_d) b_w d \quad \text{(SI units)}; \quad (9)$$

$$V_{ul} = 0.4 b_w d + \sqrt{f_c^{'} \rho_w (d/a)} (10 - 3 A_d) b_w d \quad \text{(SI units)}; \quad (10)$$

here, A_d = the shape adjustment factor ($A_d = a/d$ for $1.0 < a/d < 2.5$; $A_d = 2.5$ for $a/d \geq 2.5$).

Zsutty (1971) recognized that the shear test data are not homogeneous due to the fact that there are two distinct types of beam behavior. Accordingly, he segregated the data and performed separate regression analyses for short beams and long beams. The crack and ultimate shear strength prediction equations can be computed separately as follows

$$V_{cr} = 2.02 \left(f_c^{'} \rho_w \frac{d}{a} \right)^{1/3} b_w d \quad \text{(SI units)}; \quad (11)$$

$$V_{ul} = 2.17 \left(f_c^{'} \rho_w \frac{d}{a} \right)^{1/3} b_w d \quad \text{(SI units)}. \quad (12)$$

Eqs. (11) and (12) should be multiplied by 2.5(d/a) when $a/d < 2.5$. Both Eqs. (11) and (12) take into account the influence of the compression strength of the concrete and the longitudinal reinforcement ratio.

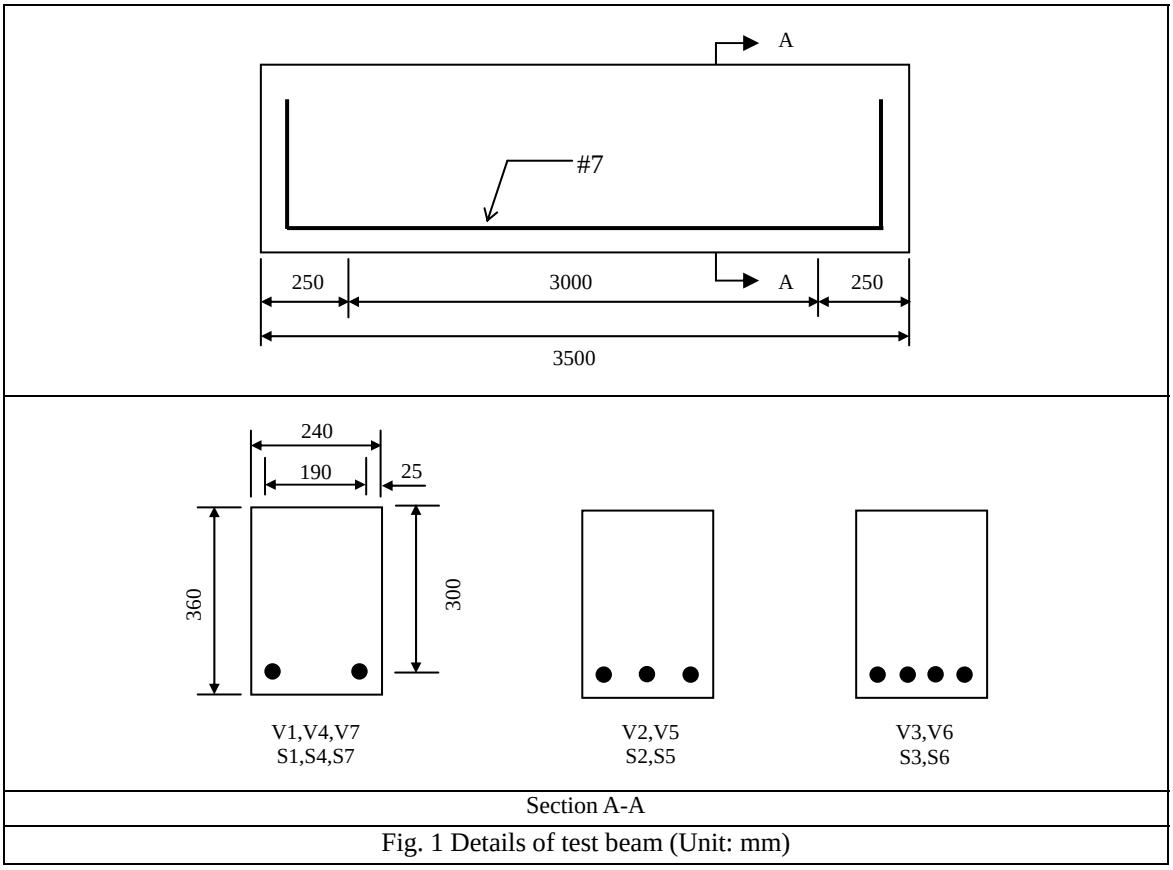

Fig. 1 Details of test beam (Unit: mm)

Table 1 Details of test specimens

Concrete type	Specimens	Cement content	f_{re}' (MPa)	b_w (mm)	d (mm)	Number/type of bottom bars	ρ_w (%)	Shear span a (mm)	a/d
Series V (LcHPC)	V1	250 (kg/m^3)	65	240	300	2-#7	1.1	900	3.0
	V2					3-#7	1.6	900	3.0
	V3					4-#7	2.2	900	3.0
	V4					2-#7	1.1	450	1.5
	V5					3-#7	1.6	450	1.5
	V6					4-#7	2.2	450	1.5
	V7					2-#7	1.1	750	2.5
Series S (HPC)	S1	350 (kg/m^3)	65	240	300	2-#7	1.1	900	3.0
	S2					3-#7	1.6	900	3.0
	S3					4-#7	2.2	900	3.0
	S4					2-#7	1.1	450	1.5
	S5					3-#7	1.6	450	1.5
	S6					4-#7	2.2	450	1.5
	S7					2-#7	1.1	750	2.5

Note: f_{re}' = 56-day design compressive strength, b_w = breadth of beam, d = effective depth of beam, ρ_w = tension reinforcement ratio and a/d = shear span to effective depth.

3. Experimental program

3.1 Test specimens

Two series of reinforced concrete beams, each having seven beams, were cast without shear reinforcements. The first series (Series V) was made with a low-cement-content high-performance concrete (LcHPC), and the other (Series S) was made with a conventional-cement-content high-performance concrete (HPC). All specimens had the same dimensions and were designed to fail in shear. Table 1 gives details of the test specimens. Fig. 1 shows the beam dimensions and reinforcement details. The beams were 240 mm wide × 360 mm deep × 3500 mm long. The clear thickness of concrete cover was selected as 25 mm. To ensure adequate anchorage, the anchorage of the longitudinal bars was maintained by extending 250 mm of extra length past the center-line of both supports and having 90-degree hooks at the beam-ends.

3.2 Materials

The locally available cementitious materials used in this research included Type-Ⅰ Portland cement, Class F fly ash and blast-furnace slag. The coarse aggregate used was crushed limestone with a maximum size of 12.7 mm, and the fine aggregate was natural river sand with a Fineness Modulus of 2.94. Table 2 shows the physical properties of the natural coarse and fine aggregates. A superplasticizer conforming to ASTM C-494 Type G was used, and enough mixing time was allowed to produce uniform mixing of the concrete without any segregation. A locally available No. 7 deformed steel bar with a nominal yield strength of 613 MPa and an ultimate tensile strength of 713 MPa was used as tension reinforcement.

3.3 Mixture proportions and fabrication of specimens

Table 3 gives the mix proportions of the two concrete series. Mixtures for both series were designed for a specified compressive strength of 65 MPa at 56 days. All aggregates were cured in a room until the required saturated surface-dry condition was reached. The treated aggregates were then stored in a room in which the ambient temperature and relative humidity (RH) were then stored in a room in which the ambient temperature and relative humidity (RH) were controlled at

Table 2 Physical properties of aggregates

Type	Specific gravity (SSD)	Water absorption (SSD)	Fineness modulus
Coarse aggregate	2.61	1.73%	5.94
Fine aggregate	2.60	1.72%	2.94

Table 3 Mix proportion of concrete

Series	W/B^*	Cement (kg/m^3)	Fly ash (kg/m^3)	Slag (kg/m^3)	Water (kg/m^3)	Fine aggregate (kg/m^3)	Coarse aggregate (kg/m^3)	SP^+ (kg/m^3)
V	0.30	250	105	197	155	628	1040	10.5
S	0.35	350	104	86	180	834	780	9.0

Note: *Water-to-binder ratio and $^+$ Superplasticizer.

25±3℃ and 50±5% to prevent moisture changes. In mixing, the cement, sand and coarse aggregates were generally blended first, and then water and superplasticizer were added. The mixing continued until a uniform concrete was obtained.

Freshly mixed concrete was then slowly poured into beam mold to a half depth across the horizontal surface and was followed by controlled vibrations. Immediately after the vibrations, the second half was poured in and was subjected to vibrations again to ensure that the concrete was well compacted. For each concrete mix, six 100-mm-diameter × 200-mm-high cylindrical specimens, referred to hereafter as control cylinders, were also cast. Following casting, all the specimens were covered overnight with a wet hessian and polyethylene sheets. Then, the beams and their respective control cylinders were removed from the molds. To maintain the same environmental conditions, all specimens were covered by wet hessian and polyethylene sheets till the time of the testing.

3.4 Instrumentation and test procedures

Fig. 2 shows the test set-up of the 500-kN servo-hydraulic material testing system designed to provide two shear spans near the support ends and a pure bending span in the middle region of a simply supported beam. The length of the shear span can be adjusted to comply with variable shear span-depth ratios. The test beams were simply supported at both ends using roller supports and were subjected to two equally spaced concentric loads through a steel spreader. The supports were fixed tightly on the rigid base by bolts. A calibrated load cell was placed between the jack and spreader beam. Linear variable displacement transducers (LVDTs) were installed to measure the mid-span displacement under increasing loads. The tests were carried out by displacement control, and the displacement rate of the actuator was maintained at 0.02 mm/sec. The test progress was monitored on a computer screen, and all load and deformation data were captured and stored in a diskette via a data logger. The diagonal crack widths of the test beam were also observed by a magnifying glass with a scale of 0.1 millimeter before a significant inclined cracking load was reached.

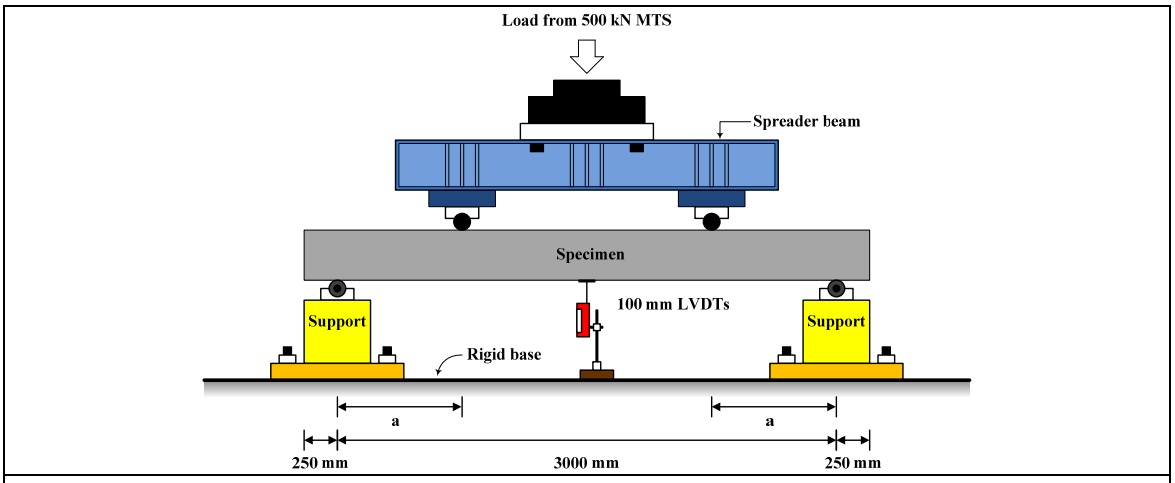

Fig. 2 Test setup

Table 4 Test results of specimens

Specimens No.	f_c' (MPa)	a/d	ρ_w (%)	V_{cr} (kN)	V_{ul} (kN)	$\frac{V_{cr}}{V_{ul}}$	Failure mode
V1	69.2	3.0	1.1	92.4	101.2	0.91	Shear-bond
V2		3.0	1.6	98.7	104.0	0.95	Shear-bond
V3		3.0	2.2	125.7	133.5	0.94	Shear-bond
V4		1.5	1.1	189.1	452.9	0.42	Shear compression
V5		1.5	1.6	217.0	512.3	0.42	Shear compression
V6		1.5	2.2	246.7	659.3	0.37	Arch-rib
V7		2.5	1.1	117.0	139.7	0.84	Shear-bond
S1	68.7	3.0	1.1	89.4	97.0	0.92	Shear-bond
S2		3.0	1.6	109.8	120.8	0.91	Shear tension
S3		3.0	2.2	110.7	123.8	0.89	Shear-bond
S4		1.5	1.1	139.7	321.4	0.43	Shear compression
S5		1.5	1.6	149.0	421.0	0.35	Shear compression
S6		1.5	2.2	178.7	437.2	0.41	Arch-rib
S7		2.5	1.1	94.2	114.2	0.82	Shear-bond

Note: f_c' = 56-day compressive strength, ρ_w = tension reinforcement ratio, a/d = shear span to effective depth, V_{cr} = measured crack shear strength and V_{ul} = measured ultimate shear strength.

4. Experimental results and discussion

4.1 Compressive strength of concrete

On the day of the beam test, the respective control cylinders were capped and tested in compression to determine the compressive strength of concrete. Mean compressive strength was calculated by taking average of six specimens. Table 4 shows that the average values of the 56-day compressive strengths are 69.2 and 68.7 MPa for Series V and S specimens, respectively. The results indicate that although the two mix designs were different, they had similar compressive strengths.

4.2 Failure modes

The test results show that all tested beams failed in shear because the strengths of the beams in diagonal tension were lower than their strengths in flexure. Basically, this study identified three failure modes. The last column in Table 4 tabulates the failure types of the tested beams. The details of the experimental results for beams with different a/d ratios are described below.

The beams with a/d values of 3.0 and 2.5 failed due to splitting along the tension reinforcement. This type of failure is referred to as “shear-bond” failure. Fig. 3(a) shows the sequence of crack formation. Vertical flexural cracks were the first to form within the mid-span region of the specimen, and the appearance of these cracks was almost instantaneous. Then, flexural cracks were observed in the shear span region, and subsequently some of the cracks developed to the mid-depth of the beam section. As the applied load continually increased, the last-formed flexural cracks extended into an inclined crack near one of the supports or a diagonal crack formed abruptly at the mid-depth of the beam within the shear span. The diagonal crack propagated toward the loading point with increasing load. However, the diagonal crack encountered resistance as it moved up into the zone of compression, became flatter and ceased its upward progression at

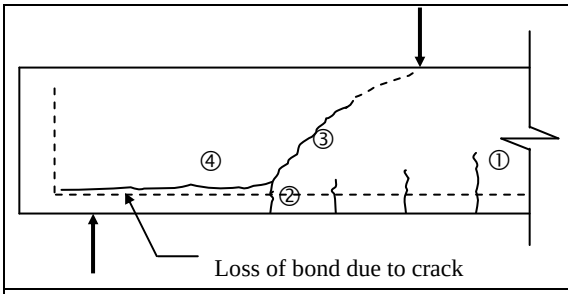

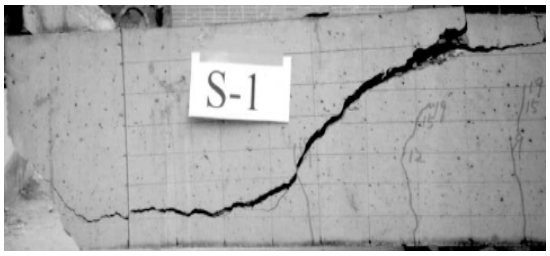

(a) Shear-bond failure

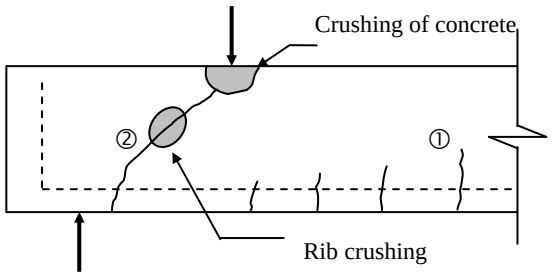

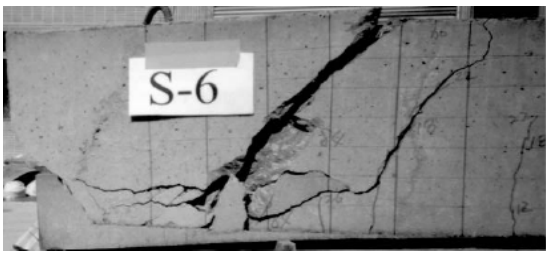

(b) Shear-compression and arch-rib failure

Fig. 3 Beam shear failure modes

some point. With further loading, the diagonal crack opened further, while a crack developed along the tension reinforcement. The reinforcement to the left of the crack was forced down, further reducing the bond between the concrete and reinforcement. With hooks provided, the beam behaved as a tied arch and failed when the concrete around the hook failed. Intrinsically, the failure load was only slightly greater than the diagonal cracking load.

For short beams with an *a/d* value of 1.5, two failure modes were identified. Fig. 3(b) shows the typical cracking patterns at failure observed in this experimental campaign. As the load on a beam increased, flexural cracks also formed within the mid-span region of the specimen. Then, a larger shear in the shear span initiated an approximately 45-degree diagonal crack across the neutral axial. As the load increased, the diagonal crack progressed into the compression zone, eventually causing the compression zone to fail explosively. This type of failure is referred to as "shear-compression" failure. However, if the vertical compressive stresses under the load reduce the possibility of further tension cracking and bond splitting along the tension reinforcement, then alternatively more cracks progress along the compressive stress trajectories in the shear span. Finally, the failure of the arch rib occurred due to a crushing of concrete on the underside of the rib. This type of failure is known as an "arch-rib" failure. Nevertheless, the failure load can be several times the load at diagonal cracking.

4.3 Load-deflection characteristics

Fig. 4 shows the plots of load versus mid-span deflection for all the tested beams. Beams made with different concrete types and *a/d* values seemed to have a common behavior of pseudo-linearity from the start of the load application to the point when the first hairline crack formed and nonlinearity afterward (see Fig. 4). Accordingly, the load-deflection relationship can

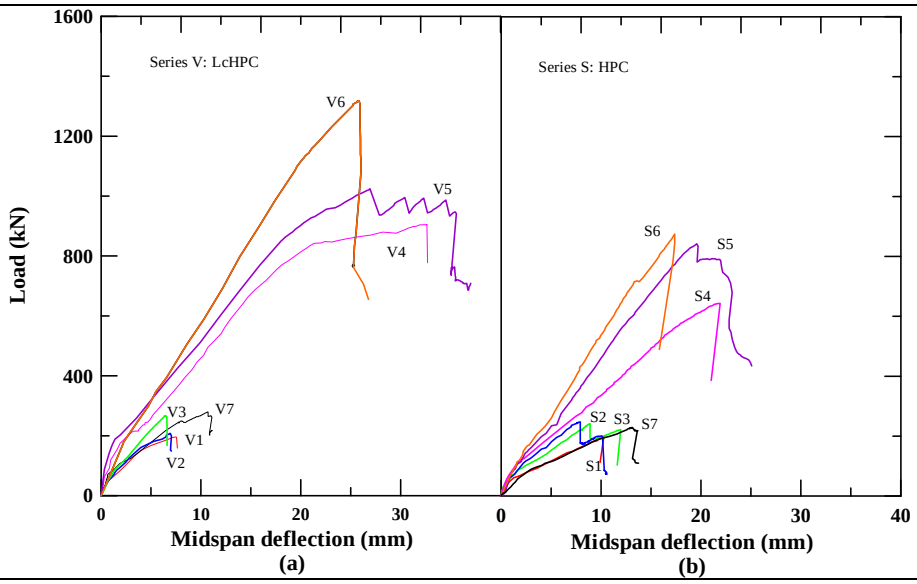

Fig. 4 Load-deflection curves

be divided into three stages. During Stage I (i.e., the pre-cracking stage), the maximum tensile stress was less than its tensile strength in flexure, which was less than the rupture modulus of concrete. Thus, the beams were crack-free, and they were observed to behave linearly from initial loading up to the occurrence of the first flexural crack. The pre-cracking stage ended at the initiation of the first crack and moved into Stage II. After cracking, the beams also exhibited a pseudo-linearity behavior but with reduced stiffness. In Stage II, the uncracked segments below the neutral axis along the beam span still possessed some degree of stiffness, contributing to the overall beam rigidity. With further loading, however, there was an obvious decrease in stiffness at a load level of about 70-90% of the ultimate load (in which the ultimate load is defined as the maximum load measured during each test), as extensive cracking occurred, and this thus led into Stage III. In this stage, the load-deflection diagram was flatter due to the substantial stiffness loss of the section. The cracks continued to open, and the neutral axis continued to rise upward until either a crack developed along the tension reinforcement or there was complete crushing of the concrete upon rupture.

Fig. 5 shows the comparison of influence of *a/d* values upon load versus mid-span deflection for LcHPC and HPC beams with a constant ρ_w. The slope of the pre-peak stage was steeper for LcHPC beams with an *a/d* value of 1.5 as compared with those with *a/d* values of 2.5 and 3.0. In addition, Fig. 5 shows that under a constant ρ_w, as the *a/d* value decreases from 3.0 to 1.5, the ultimate loads for LcHPC beam wereclearly increased. Similar behavior was observed for beams made of HPC with a conventional cement content. This behavior is attributed to the fact that beams with *a/d* = 1.5 developed inclined compression struts, inducing an arching action within the shear span of a test beam. In other words, despite the appearance of a diagonal crack, the specimen exhibited significant load-carrying capacity through the compressive strut. In general, smaller *a/d* values meant higher ultimate strengths. For example, in LcHPC beams, the increased load is significant, with the ultimate load over four times as much for *a/d* = 1.5 as compared to *a/d* = 3.0.

The effects of ρ_w on load versus mid-span deflection are shown in Figs. 6 through 8 for both

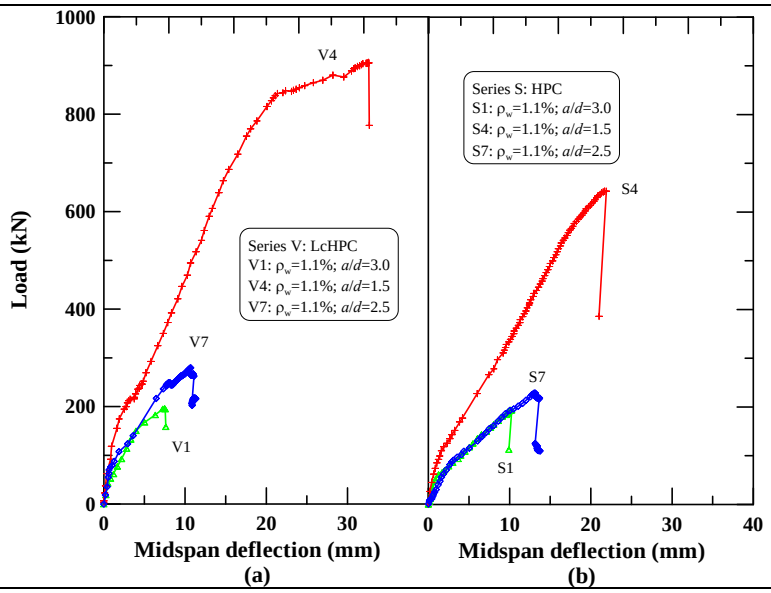

Fig. 5 Influence of *a/d* ratios upon load-deflection curves

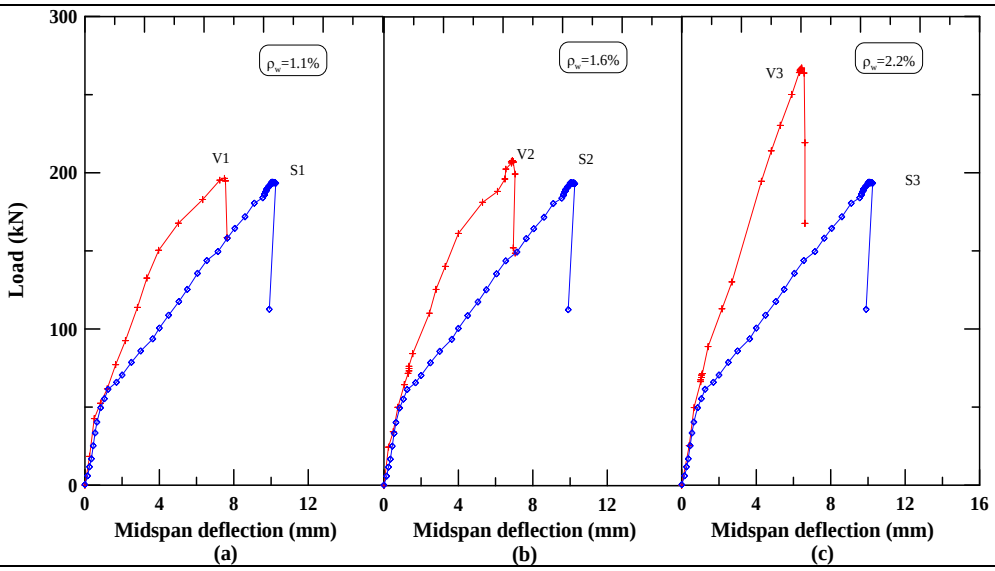

Fig. 6 Influence of ρ_w upon load-deflection curves (with *a/d*=3.0)

series (V and S) of beams subjected to various values of *a/d*. The beams with high values of ρ_w obviously had stiffer responses to loading in the pre-peak stage than those of lower values (see Fig. 6). This stiffer response occurs because the moment of inertia of the uncracked beam gross cross-section in Stage I and the effective moment of inertia of the cracked beam gross cross-section in Stage II, including the tensile reinforcement stiffness, increase with the increase of ρ_w. Accordingly, greater values of ρ_w indicate steeper slopes of the pre-peak stage. Furthermore, in

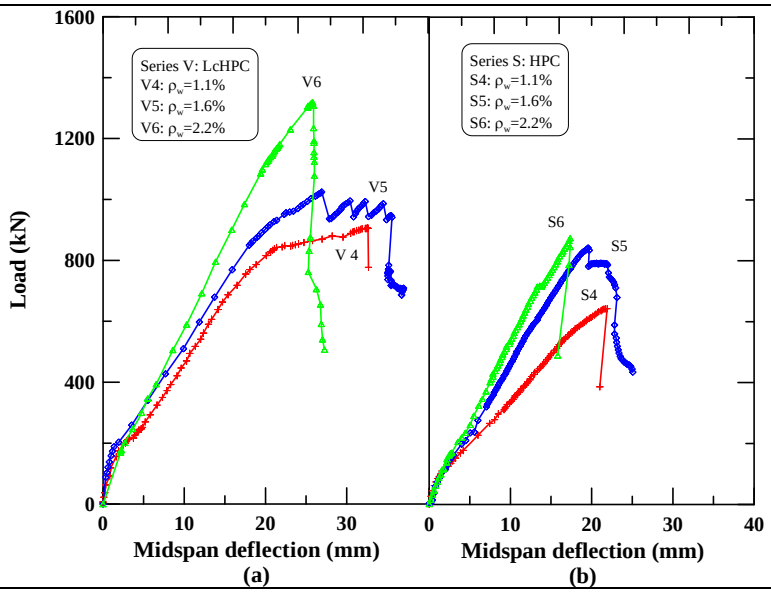

Fig. 7 Influence of ρ_w upon load-deflection curves (with a/d=1.5)

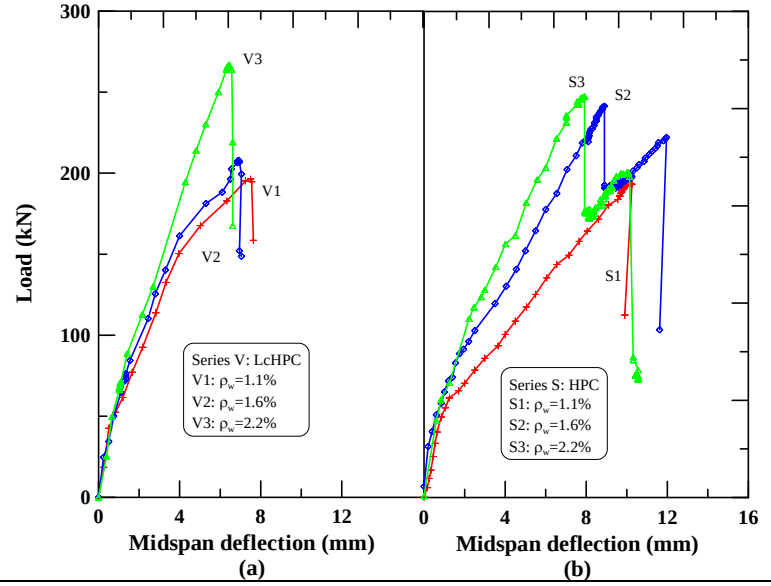

Fig. 8 Influence of ρ_w upon load-deflection curves (with a/d=3.0)

comparing any two beams with nearly the same concrete strength, Figs. 6 through 8 shows that the beam with the higher tensile reinforcement content endured less deformation for the same magnitude of load. However, the slopes of the ascending portions of load-displacement curves for the LcHPC beams were steeper than those for the HPC beams with the same strength grades under fixed a/d values (see Fig. 6). This behavior is because that there was a higher coarse aggregate content of the mix in the LcHPC as compared with the HPC, and thus a higher elastic modulus and stiffness might be achieved for the LcHPC (Table 3).

4.4 Crack shear strength and ultimate shear strength

The crack shear strength, V_{cr}, which is defined as the shear causing significant inclined cracking, was determined from the corresponding load and mid-span deflection curve as the first point of curvature change or where the load was suddenly decreased. The ultimate shear strength, V_{ul}, which is defined as the shear strength when complete and total failure occurs, was also measured.

Due to differences in the failure mechanisms, the shear strength of beams with a/d = 3.0 was much less than those of beams with a/d of 1.5 and 2.5. The measured V_{cr} and V_{ul} are summarized in Table 4 for both series of beams. As shown in Table 4, beams with LcHPC (except beam V2) have higher crack and ultimate shear strengths than corresponding HPC beams. Generally, Table 4 shows that the difference was less significant between the crack shear strengths of the specimens made with the two different types of concrete for beams with a/d = 3.0. However, the failure mechanism of the compression zone changed from a tension failure to a compression failure as the

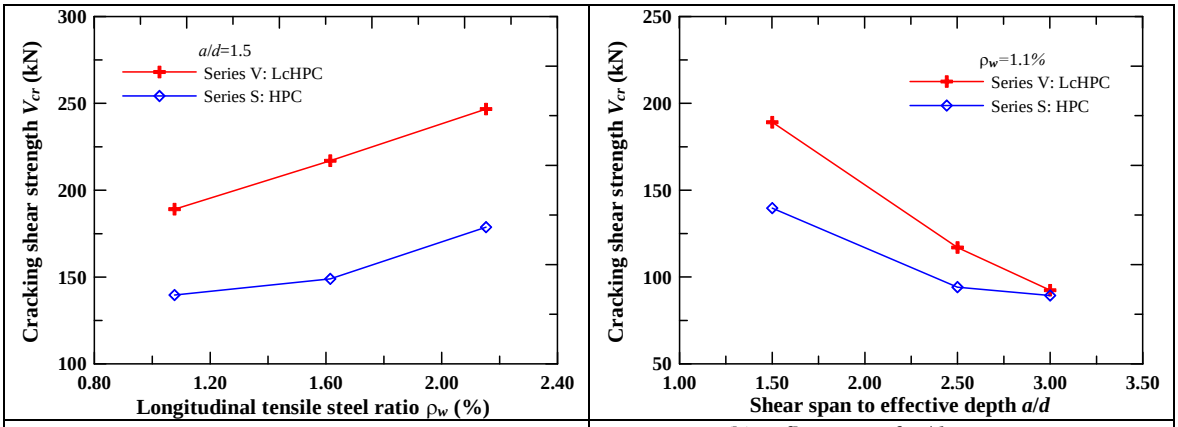

(a) Influences of ρ_w upon V_{cr} (b) Influences of a/d upon V_{cr}

Fig. 9 Influences of ρ_w and a/d upon V_{cr}

Table 5 Comparison of shear strengths

Specimens No.	V_{cr} (kN)	V_{ul} (kN)	Specimens No.	V_{cr} (kN)	V_{ul} (kN)	$\frac{V_{cr,LcHPC}}{V_{cr,HPC}}$	$\frac{V_{ul,LcHPC}}{V_{ul,HPC}}$
V1	92.4	101.2	S1	89.4	97.0	1.03	1.04
V2	98.7	104.0	S2	109.8	120.8	0.90	0.86
V3	125.7	133.5	S3	110.7	123.8	1.14	1.08
V4	189.1	452.9	S4	139.7	321.4	1.35	1.41
V5	217.0	512.3	S5	149.0	421.0	1.46	1.22
V6	246.7	659.3	S6	178.7	437.2	1.38	1.51
V7	117.0	139.7	S7	94.2	114.2	1.24	1.22
Average						1.21	1.19

Note: $V_{cr,LcHPC}$=measured crack shear strength of LcHPC beams, $V_{ul,LcHPC}$=measured ultimate shear strength of LcHPC beams, $V_{cr,\ HPC}$=measured crack shear strength of HPC beams and $V_{ul,HPC}$=measured ultimate shear strength of HPC beams.

a/d ratio decreased. Especially for the beam with *a/d* = 1.5, the failure mechanism was governed mainly by the properties of the concrete. The crack shear strengths of the LcHPC beams were evidently larger than those of the corresponding HPC beams due to a larger aggregate content in the LcHPC mix design. Table 5 shows that the measured V_{cr} of the LcHPC and the HPC beams. The average ratio of $V_{cr,LcHPC}/V_{cr,HPC}$ is 1.21. In addition, the crack shear strength of both series of beams increased with the increase of ρ_w, whereas it decreased with the increase of *a/d* value (see Fig. 9).

Furthermore, Table 5 shows that the measured V_{ul} of the LcHPC and the HPC beams. The average ratio of $V_{ul,LcHPC}/V_{ul,HPC}$ is 1.19. The influences of ρ_w and *a/d* on the ultimate shear strength are shown in Fig. 10. Likewise, the ultimate shear strength of both series of beams increased with the increase of ρ_w, whereas it decreased with the increase of *a/d* value.

4.5 Comparison of test results with empirical shear strength equations

Table 6 Comparison between experimental and calculated ultimate shear strengths

Specimens No.	$\frac{V_{ul}}{V_{ACI,D}}$	$\frac{V_{ul}}{V_{ACI,STM}}$	$\frac{V_{ul}}{V_{ul,EC02}}$	$\frac{V_{ul}}{V_{ul,Zsutty}}$	$\frac{V_{ul}}{V_{ul,Rebeiz}}$
V1	1.01	-	1.02	1.03	0.85
V2	1.02	-	0.92	0.92	0.75
V3	1.28	-	1.10	1.08	0.86
V4	4.33	1.79	4.57	2.20	1.18
V5	4.70	1.34	4.52	2.17	1.10
V6	5.81	1.32	5.41	2.54	1.24
V7	1.38	-	1.41	1.03	0.85
AVE	2.79	-	2.71	1.61	1.01
COV	0.74	-	0.75	0.41	0.19
Specimens No.	$\frac{V_{ul}}{V_{ACI,D}}$	$\frac{V_{ul}}{V_{ACI,STM}}$	$\frac{V_{ul}}{V_{ul,EC02}}$	$\frac{V_{ul}}{V_{ul,Zsutty}}$	$\frac{V_{ul}}{V_{ul,Rebeiz}}$
S1	0.97	-	0.98	0.99	0.82
S2	1.18	-	1.07	1.08	0.87
S3	1.19	-	1.02	1.00	0.80
S4	3.08	1.27	3.25	1.56	0.84
S5	3.87	1.11	3.72	1.79	0.91
S6	3.87	0.88	3.60	1.69	0.83
S7	1.13	-	1.16	1.10	0.90
AVE	2.19	-	2.11	1.31	0.85
COV	0.62	-	0.63	0.27	0.05

Note: AVE=average of $V_{ul,test}/V_{ul,calc}$, COV=coefficient of variation of $V_{ul,test}/V_{ul,calc}$, $V_{ul,test}$=measured ultimate shear strength, $V_{ACI,D}$=calculated shear strength by Eq. (2), $V_{ACI,STM}$=calculated shear strength using the strut-and-tie method (STM) given in Appendix A of the ACI 318-08 Code, $V_{ul,EC02}$=calculated shear strength by Eq. (8), $V_{ul,Zsutty}$=calculated shear strength by Eq. (12) and $V_{ul,Rebeiz}$=calculated shear strength by Eq. (10).

The ratio between the experimental crack shear strength, $V_{cr,test}$, and the calculated crack shear

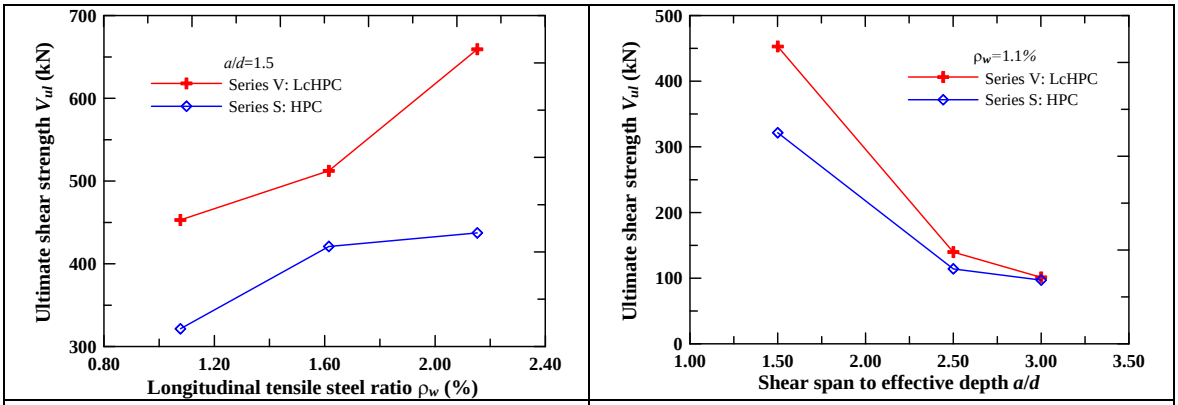

(a) Influences of ρ_w upon V_{ul} (b) Influences of a/d upon V_{ul}

Fig. 10 Influences of ρ_w and a/d upon V_{ul}

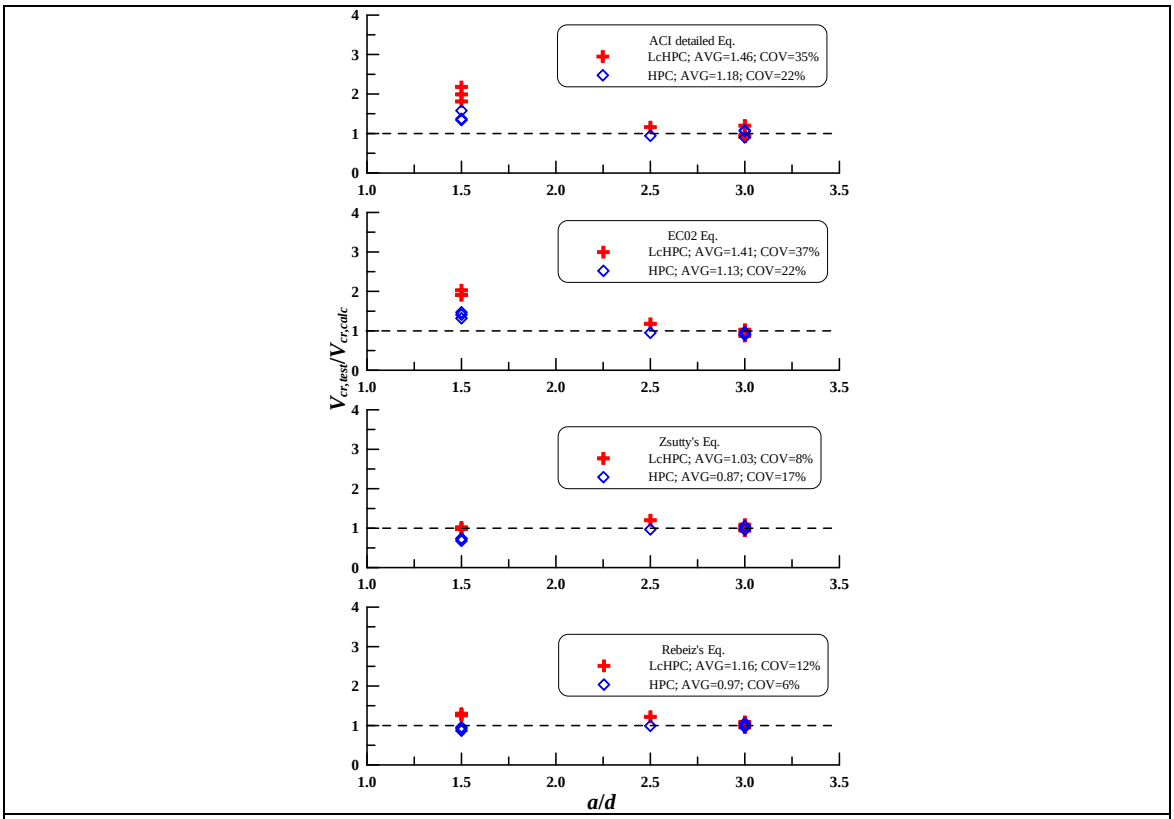

Fig. 11 Relations of $V_{cr,test}/V_{cr}$ and a/d ratio

strength, $V_{cr,calc}$, by means of Eqs. (1) to (4) is plotted versus the shear span to effective depth ratio, as shown in Fig. 11. The minor scatter of data around the horizontal dashed line confirms that Zsutty's equation and Rebeiz's equation are excellent predictors for the crack shear strength of

both series of beams. However, the correlation between the values of $V_{cr,test}$ and $V_{cr,calc}$, which were obtained from Eqs. (2) and (4), is more scattered. The test results clearly indicate that shear span to effective depth ratio *a/d* has the most significant influence on the behavior of the tested beams. However, the simplified ACI equation, Eq. (1), gives a constant value of strength irrespective of *a/d*. In contrast, the detailed ACI equation, Eq. (2), accounts very conservatively for the effect of *a/d*.

Table 6 shows the comparison between the experimental ultimate shear strength, $V_{ul,test}$, and the calculated ultimate shear strength, $V_{ul,calc}$, that was calculated by using the aforementioned empirical formulae. This table also tabulates the average ratio, $V_{ul,test}/V_{ul,calc}$, and the corresponding coefficient of variation (COV) for both series of beams. Both Eqs. (2) and (8) definitely underestimate the ultimate shear strength. The reason for this underestimation is that these equations are used to predict the crack shear strength, which is a shear strength at the occurrence of a first major diagonal crack. However, the measured ultimate shear strength is defined as the shear strength when complete and total failure occurs. Thus, based on this experimental study, it can be expected that the ACI code prediction regarding the ultimate shear strength of the beam is very conservative for both series of beams with *a/d* ratios within the limits of 1.5 to 2.5. Therefore, for deep beams with an *a/d* ratio of 1.5, the measured ultimate shear strength is compared with the calculated ultimate shear strength using the strut-and-tie method given in Appendix A of the ACI 318-08 Code. Table 6 shows that the STM gives a better representation of the load–carrying mechanism at failure in deep beams. In addition, the values of $V_{ul,test}/V_{ul,calc}$ of Rebeiz's equation were much better than those of Eqs. (2), (8) and (12). For LcHPC beams, the average and coefficient of variation of $V_{ul,test}/V_{ul,calc}$ are 1.01 and 19%, respectively, and the correlation ratio ranges from 0.75 to 1.24. In other words, Table 6 shows that Rebeiz's equation is a comparatively proper predictor of the ultimate shear strength of tested beams.

5. Conclusions

The shear strength and cracking behavior of LcHPC beams were described and compared with companion HPC beams. The influences of material parameters, the shear span to effective depth ratio, and the tensile steel ratio on the crack load, failure modes and overall shear resistance at failure were thoroughly analyzed. Based on the experimental results, the following conclusions can be drawn:

1. The anticipated shear failure of the LcHPC beams without shear reinforcements tends to be brittle. Beams with an *a/d* value of 1.5 under design loads mostly fail in concrete crushing above the inclined cracks, whereas beams with an *a/d* value of 3.0 may fail by bond failure attributed to the splitting of bonds along the tension reinforcement.
2. The slopes of the ascending segment of load-displacement curves for the LcHPC beams are steeper than those of companion HPC beams with the same *a/d* values due to the different aggregate contents for the two mix designs.
3. The ACI equations are quite conservative in predicting the crack shear strength for both the LcHPC beams and HPC beams, especially with an *a/d* value of 1.5, whereas Zsutty's and Rebeiz's equations correlate reasonably well with the test results.
4. The detailed ACI equation and the STM given in Appendix A of the ACI 318-08 Code are conservative in predicting the ultimate shear strength for both the LcHPC beams and HPC beams with an *a/d* value of 1.5, whereas Rebeiz's equation is a comparatively proper predictor of the

ultimate shear strength of all the beams.

Acknowledgments

The authors express their gratitude and sincere appreciation to the authority of National Science Council, Taiwan, for financing this research work.

References

ACI Committee 318 (2008), *Building code requirements for structural concrete (ACI 318-08) and commentary*, American Concrete Intitute, Farmington Hills, Mich.

Bentz, E.C. (2005), "Empirical modeling of reinforced concrete shear strength size effect for members without stirrups", *ACI Struct. J.*, **102**(2), 232-241.

Chen, H.J., Yang, T.Y. and Tang, C.W. (2009), "Strength and durability of concrete in hot spring environments", *Comput. Concrete*, **6**(4), 269-280.

Cho, S.H. (2003), "Shear strength prediction by modified plasticity theory for short beams", *ACI Struct. J.*, **100**(1), 105-112.

Choi, K.K., Park, H.G. and Wight, J.K. (2007), "Unified shear strength model for reinforced concrete beams-Part I: Development", *ACI Struct. J.*, **104**(2), 142-152.

ENV 1992-1-1: Eurocode No. 2. (1991), *Design of concrete structures- Part 1: General rules and rules for building*, Commission of the European Communities.

Hassan, A.A.A., Hossain, K.M.A. and Lachemi, M. (2008), "Behavior of full-scale self-consolidating concrete beams in shear", *Cement Concrete Comp*., **30**(7), 588-596.

Mehta, P.K. and Monteiro, P.J.M. (2006), *Concrete: Microstructure, properties, and materials* (International Editions 2006), McGraw-Hill Education (Asia), Taiwan.

Park, R. and Paulay, T. (1975), *Reinforced concrete structures*, John Wiley & Sons.

Somayaji, S. (2001), *Civil engineering materials*, Prentice Hall, Upper Siddle River, New Jersey.

Tang, C.W., Yen, T. and Chen, H.J. (2009), "Shear behavior of reinforced concrete beams made with sedimentary lightweight aggregate without shear reinforcement", *J. Mater. Civil Eng.-ASCE*, **21**(12), 730-739.

Tang, C.W. (2010), "Hydration properties of cement pastes containing high-volume mineral admixtures", *Comput. Concrete*, **7**(1), 17-38.

Taylor, H.P.J. (1972), "Shear strength of large beams", *J. Struct. Div.-ASCE*, **98**(11), 2473-2490.

Rebeiz, K.S. (1999), "Shear strength prediction for concrete members", *J. Struct. Eng.-ASCE*, **125**(3), 301-308.

Russell, H.G. (1999), "ACI defines high performance concrete", *Concrete Int.*, **21**(2), 56-57.

Russo, G., Somma, G. and Mitri, D. (2005), "Shear strength analysis and prediction for reinforced concrete beams without shear stirrups", *J. Struct. Eng.-ASCE*, **131**(1), 66-74.

Zarais, P.D. and Papadakis, G.C. (2001), "Diagonal shear failure and size effect in RC beams without web reinforcement", *J. Struct. Eng.-ASCE*, **127**(7), 733-742.

Zararis, P.D. (2003), "Shear strength and minimum shear reinforcement of reinforced concrete slender beams", *ACI Struct. J.*, **100**(2), 203-214.

Zsutty, T.C. (1971), "Shear strength prediction for separate categories of simple beam test", *ACI J.*, **68**(2), 138-143.